gels

MDPI

Article

The enrichment of whey protein isolate hydrogels with Poly-γ-glutamic acid promotes the proliferation and osteogenic differentiation of pre-osteoblasts

Daniel K. Baines [1,2], Varvara Platania [3], Nikoleta N. Tavernaraki [3], Mattia Parati [4], Karen Wright [2], Iza Radecka [4], Maria Chatzinikolaidou [3,5], Timothy E. L. Douglas [1]*

[1] School of Engineering Lancaster University, Gillow Avenue, Lancaster LA1 4YW, UK; d.baines3@lancaster.ac.uk
[2] Biomedical and Life Sciences Lancaster University, Gillow Avenue, Lancaster LA1 4YW, UK; d.baines3@lancaster.ac.uk; karen.wright@lancaster.ac.uk
[3] Department of Materials Science and Technology, University of Crete, Heraklion, Greece; mchatzin@materials.uoc.gr; plataniavarvara@yahoo.com, ntav@materials.uoc.gr
[4] Faculty of Science and Engineering, School of Life Sciences, University of Wolverhampton, United Kingdom; I.Radecka@wlv.ac.uk; M.Parati@wlv.ac.uk
[5] Institute of Electronic Structure and Laser, Foundation for Research and Technology Hellas, Heraklion, Greece
* Correspondence: t.douglas@lancaster.ac.uk

Abstract: Osseous disease accounts for over half of chronic pathologies but there is a limited supply of autografts, the gold standard, hence there is a demand for new synthetic biomaterials. Herein, we present the use of a promising new dairy-derived biomaterial, whey protein isolate (WPI) in the form of hydrogels, modified with the addition of different concentrations of the biotechnologically produced protein-like polymeric substance poly-γ-glutamic acid (γ-PGA) as a potential scaffold for tissue regeneration. Raman spectroscopic analysis demonstrated the successful creation of WPI- γ-PGA hydrogels. Cytotoxicity assessment using pre-osteoblastic cells demonstrated that the hydrogels were non-cytotoxic and supported cell proliferation from day 3 to 14. All γ-PGA -containing scaffold compositions strongly promoted cell attachment and formation of dense interconnected cell layers. Cell viability was significantly increased on γ-PGA-containing scaffolds on day 14 compared to WPI control scaffolds. Significantly, the cells showed markers of osteogenic differentiation; they synthesised increasing amounts of collagen over time; cells showed significantly enhanced alkaline phosphatase activity at day 7 and higher levels of calcium for matrix mineralization at days 14 and 21 on γ-PGA-containing scaffolds. These results demonstrated the potential of WPI- γ-PGA hydrogels as scaffolds for bone regeneration.

Keywords: Whey protein; γ-PGA; bone scaffolds; Raman; swelling; biocompatibility; ALP; collagen; osteogenesis; osteogenic differentiation; bone tissue engineering.

Citation: To be added by editorial staff during production.

Academic Editor: Firstname Lastname

Received: date
Revised: date
Accepted: date
Published: date

1. Introduction

Osseous associated defects are one group of chronic diseases, accounting for half of the chronic pathologies in individuals aged over 50 and affecting around 200 million people worldwide [1]. They are normally the result of fractures, a consequence of weakened bones caused by age-related osteoporosis [2]. Although bone possesses regenerative qualities, the possibilities are limited. Larger defects result in impaired healing and failure to regenerate significant gaps in the bone [3]. Bone autografts are the gold standard treatment [4]; however, the use of autografts present limitations including limited availability, donor site morbidity and long operation times [5]. Additionally, immune rejection and non-union present further complications [6]. Therefore, there is a requirement for scaffold

forming materials allowing for bone regeneration, resulting in the emergence of tissue engineering as a promising alternative to autologous bone grafting [7]. Potential polymers to be utilised as osteogenic scaffolds, whether natural or synthetic polymers, require certain properties. Ideally, any scaffold should share properties similar in composition, structure, and functionality to the extracellular matrix (ECM) [8]. The polymers should be bioactive, compatible, and degradable, load bearing, osteoconductive and have the potential for localised drug delivery [9]. Numerous natural or synthetic polymers have been developed including hybrid materials. However, many fail to meet all requirements for use in bone tissue engineering. They fail to produce satisfactory mechanical properties or fail to be biologically active [10, 11]. Nevertheless, a promising new biomaterial, whey protein isolate (WPI) has proven to be a potential candidate for osteo support and regeneration.

Formally, WPI is derived from a waste product of the dairy industry and contains purified proteins of whey with the main component being β-lactoglobulin, which is shown in Figure 1 [12]. The main potential of WPI as a biomaterial comes from the ability of WPI to produce pliable and sterilisable hydrogels through heat or pressure induction [13, 14]. One of the advantages of a hydrogel is the ease of incorporation of water-soluble molecules in the water phase. Although WPI does support cell attachment and proliferation, most studies have involved the formation of hybrid composites with the hydrogels. For instance, in [15] cyto-compatible WPI-bioactive glass composites were produced, supporting MG-63 osteoblasts cellular functioning. In [16] WPI-phloroglucinol (WPI-PG) hydrogels were synthesized, demonstrating that WPI-PG hydrogels support the growth of human dental pulp stem cells and osteosarcoma-derived MG-63 cells. Hence, such WPI-PG hydrogels may provide a medicinal route to restrict microbial infections, whilst presenting desirable mechanical properties and promoting stem-cell attachment. Similarly, osteogenic behaviour was observed in [17] in which WPI-hydroxyapatite hydrogels were synthesized as a potential scaffold for bone substitution. Furthermore, WPI-aragonite composites produced ECM like mineralisation and enabled MG-63 proliferation [18].

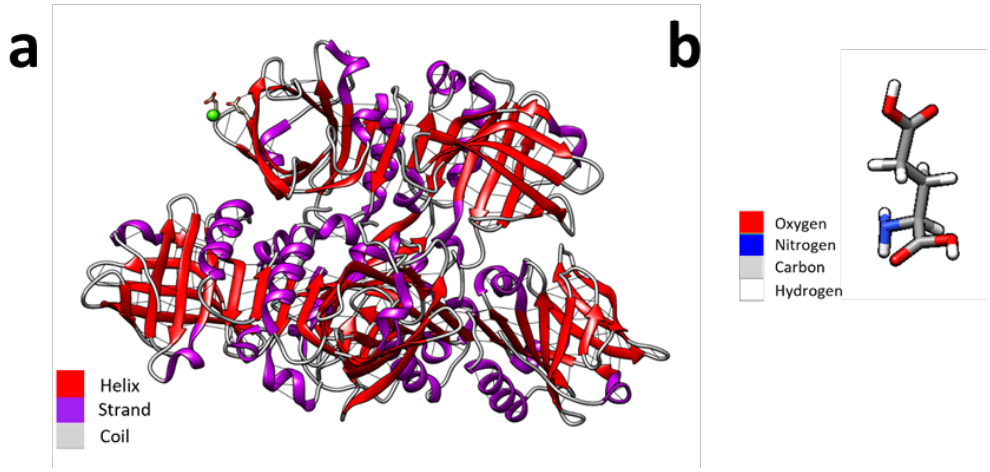

Figure 1. a) coloured depiction of the secondary structures of beta-lactoglobulin.. However, here the helix is depicted as red, strands in purple and the coils in grey. b) a glutamic acid monomer coloured by element, oxygen in red, nitrogen in blue, carbon in grey and hydrogen in white. Molecular graphics and analyses performed with UCSF Chimera [19] The beta-lactoglobulin molecular structure was sourced from PubMed and the glutamic acid molecule from PubChem.

Poly-γ-glutamic acid (γ-PGA) is a biopolymer produced primarily by bacterial gram-positive bacteria predominately those of *Bacillus* species [20]. γ-PGA was first identified in a capsule of *Bacillus anthracis*. Subsequently, it was isolated from several other microbes such as *Bacillus licheniformis*, *Bacillus subtilis natto*, *Rhodopirellula baltica* as well as *Staphylococcus epidermidis*. The mechanism of bacterial synthesis can be observed in Figure 2. The polymer consists of multiple repeating l-glutamic acid and d-glutamic acid amino acid

monomers [21]. The hydrophilic polymer has multiple interesting qualities including immunogenicity, non-toxicity and biodegradability [22]. Previously, γ-PGA has demonstrated functions compatible with osteoblastic cellular proliferation. For instance, γ-PGA combined with bioactive glass was found to have a supporting role for SaOs-2 osteosarcoma cell proliferation [23]. Recently, Parati et al. [24] demonstrated a protective role of γ-PGA on tooth enamel providing an inhibitory effect on calcium dissolution, significantly reducing the loss of hydroxyapatite.

It would be beneficial if a scaffold would prevent microbial infection. γ-PGA has demonstrated antimicrobial activity with Zu et al [25] suggesting γ-PGA demonstrates a minimum inhibitory concentration of <2.5mg/mL against Gram positive and negative species of bacteria *B. subtilis* and *Escherichia coli*, respectively. However, the present antimicrobial activity was molecular mass dependent [26]. Previously, Gamarra-montes et al [26] had demonstrated the antibacterial properties of γ-PGA against *S. aureus*, *L. monocytogenes*, *E. coli* and *P. aeruginosa*, known infection causative agents.

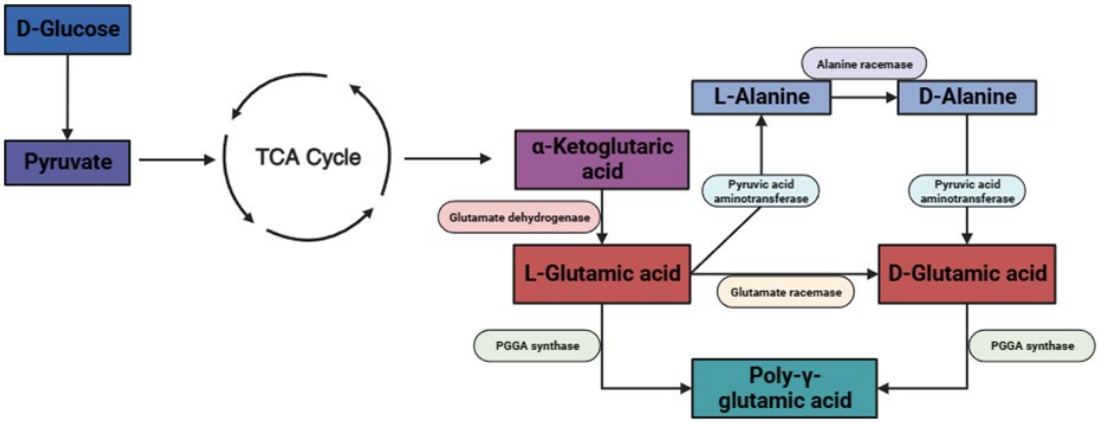

Figure 2. A schematic of the bacterial metabolic production of *γ-PGA* via the citric acid cycle (TCA). The image was created on Biorender.com.

In this study, a novel approach was taken; WPI hydrogels were combined with γ-PGA to evaluate any potential for WPI- γ-PGA hydrogels to be utilised as scaffolds for bone regeneration. Raman spectroscopy was utilised to ascertain the incorporation of γ-PGA into the WPI. Swelling assays and mechanical testing were performed to determine whether the addition of γ-PGA influences the structural behaviour of the hydrogels. Additionally, a cytocompatibility assessment was performed to determine the adhesion, viability and proliferation of pre-osteoblastic cells cultured onto hydrogels, and expression of bone-related markers was evaluated to demonstrate potential of the hydrogels to promote osteogenic differentiation.

2. Results and Discussion

2.1. Raman Spectroscopy

Raman spectroscopy was employed to ascertain the incorporation of glutamic acid polymer into the WPI hydrogel, the results of which can be observed in Figures 3, 4 and 5. A search in literature returned several peaks directly associated with glutamic acid whether that be the L or D isomers of the molecule. The peaks acquired from literature formed the basis of the analysis for the results. Although, WPI itself has glutamic acid present and thus glutamic acid associated peaks would be present, an increase in the glutamic acid associated peaks represented a positive result. Additionally, R-squared values and Lorentzian fitting was utilised to determine the statistical viability of the results. The results from the Lorentzian fitting are observable in Figure 3 a and b. Additionally, the acquired peaks post convergence can be observed in Figure 4a-d.

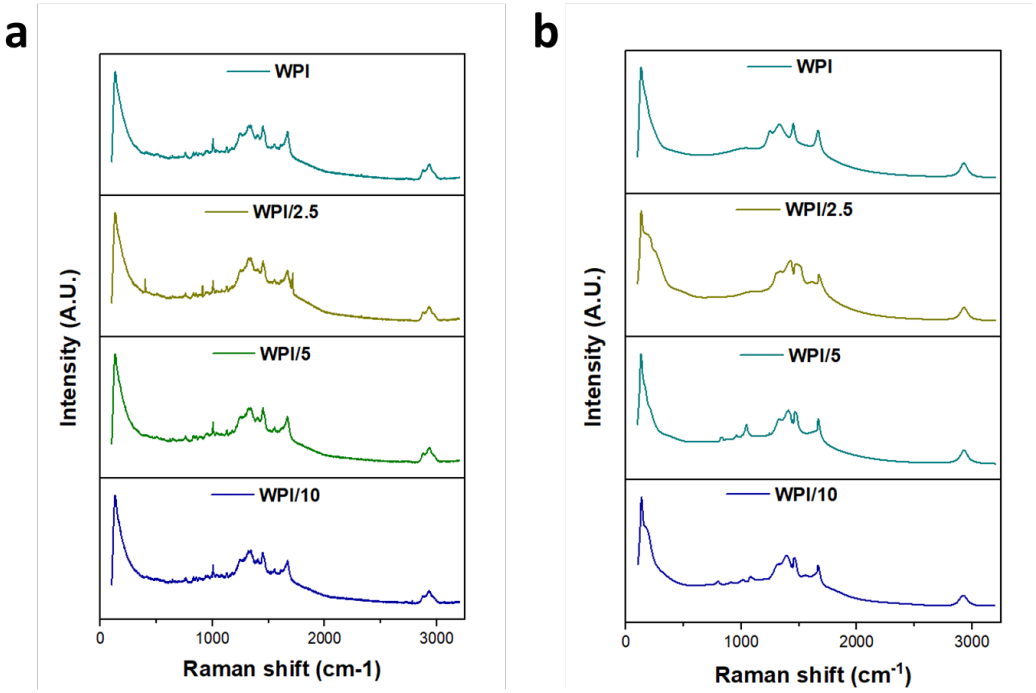

Figure 3. a and b depict Raman spectroscopy analysis pre and post normalisation observable in ascending order denoted by their γ-PGA concentration WPI = 0%, WPI/2.5 = 2.5%, WPI/5 =5% and WPI/10 =10% γ-PGA (n=5).

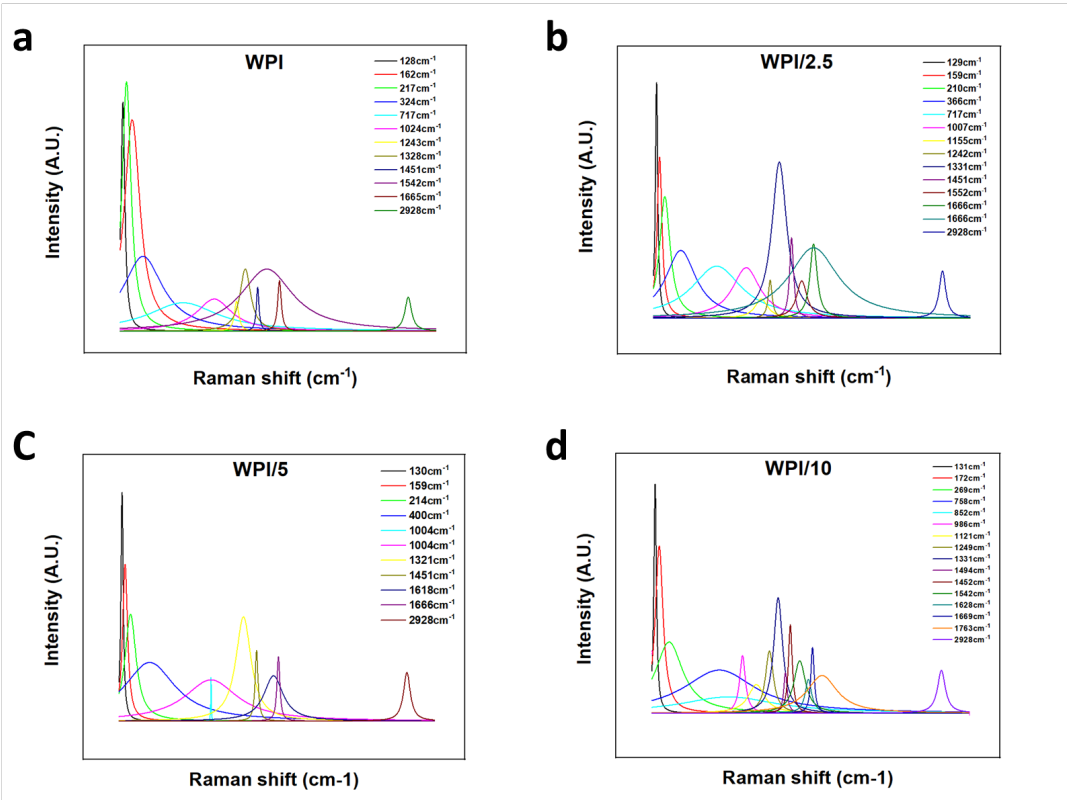

Figure 4. a-d relevant peak post convergence. The peak demonstrated the underlying molecular interactions which form the associated peaks displayed by the Raman spectroscopy results. Confidence in the results was demonstrated through Chi- squared and R squared values a – 0.99619 (CHI^2 1.16768E-4), b – 0.98978 (CHI^2 – 3.64211E-4), c – 0.9937 (CHI^2 1.94365E-4) and d – 0.99387 (CHI^2 1.80616E-4).

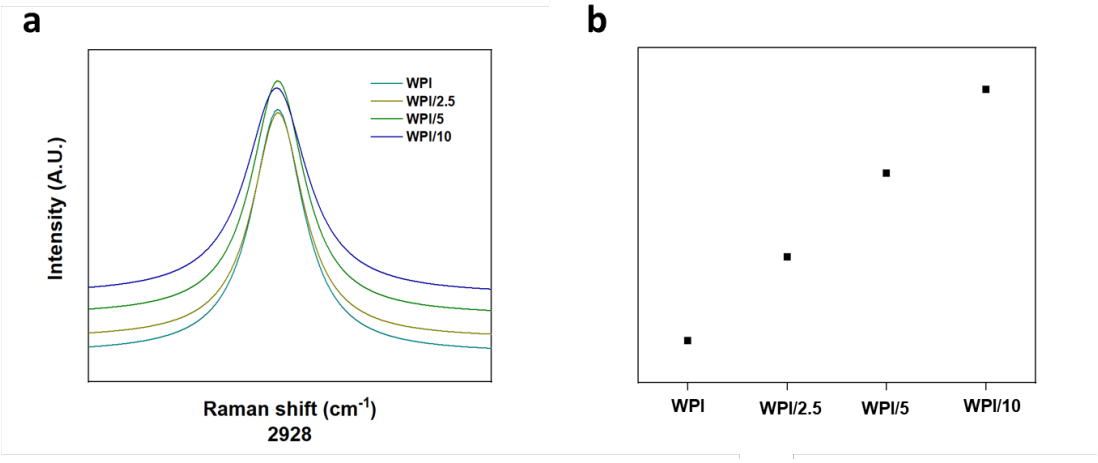

Figure 5. (a and b) depicts an example of the peaks broadening with increasing γ-PGA concentration at 2928cm^{-1}. The observables are WPI-γ-PGA concentration variables WPI = 0% γ-PGA, WPI/2.5 = 2.5% γ-PGA, 5WPI/5 = 5% γ-PGA and WPI/10 = 10% γ-PGA.

The results yielded 7 peaks that were consistent throughout all γ-PGA concentrations and 4 peaks that converged for only 1 or more of the γ-PGA concentration variables. Table 1 is representative of these results.

Table 1. Suggested underlying interactions in the γ-PGA -WPI Raman spectroscopy results.

WPI	WPI/2.5	WPI/5	WPI/10%	Interaction	Reference
128	129	130	131	Lattice rocking vibrations	[27]
162	159	159	172	CO_2 torsion, Lattice rocking vibrations	[27]
217	210	214	269	L-glutamic acid skeleton vibrations	[27]
			758-852	CH_2 rocking vibrations, COOH deformation vibrations	[28]
1024	1007	1004	986	CC stretching vibrations, C-C-N stretching vibrations	[27], [29]
	1155		1121	NH_{3+} rocking vibrations, C-O stretching vibrations, CH_2 twisting vibrations	[27], [28]
1243	1242		1249	C-O stretching vibrations, CH3 wagging vibrations, COH in plane bending vibrations, CH_3COOH (H-bonded)	[28]
1328	1331	1321	1331	COH in plane bending vibrations, CH_3 wagging vibrations, CH in plane bending vibrations, COO- symmetric stretching vibrations	[28], [29]
1451	1451	1451	1494	CH_3 antisymmetric in plane bending vibrations, COO- symmetric stretching vibrations, COH in plane bending vibrations	[28], [29]
1542	1552		1542	COO- anti-symmetric stretching vibrations	[28]
1665	1666	1666	1669/1763	C=O stretching vibrations	[27]
2928	2928	2928	2928	CH2 stretching vibrations	[27]

One glutamic acid associated peak consistent throughout all γ-PGA concentration variables was present at 2928cm^{-1}; this was representative of CH2 stretching vibrations. No Raman shift was observed between any of the WPI- γ-PGA concentration variables and the results were consistent with peaks suggested by Freire et al [27]. However, Freire

et al, suggested two strong peaks at 2938 cm^{-1} and 2974 cm^{-1} . Here we attained one strong peak at 2928 cm^{-1} suggesting a potential red shift from the 2938 cm^{-1} peaks suggested in [27]. Additionally, in [27] the L-isomer of glutamic acid was analysed specifically. Considering that γ-PGA is a complex of both D and L-isomers there was potential for the results to include interactions or spectra from the D-isomer contributing to the results with the additional interactions from the further amino acids constituent in WPI. Furthermore, as highlighted by figure 5 (a and b) red shift was observed, as expected, with an increase in γ-PGA concentration, as demonstrated by the broadening of the peaks with an increase in γ-PGA.

At the opposite end of the spectrum were peaks associated with lattice rocking vibrations, again consistent with the results from Barth et al [28], which were ascertained located below 199cm^{-1}. However, blue shift was observed with each increasing concentration variable increase 1 cm^{-1} respectively to the closest lesser concentration. For instance, the WPI-0 γ-PGA variable returned results of 128 cm^{-1}, WPI-2.5% γ-PGA 129 cm^{-1}, WPI-5% γ-PGA 130 cm^{-1} and the WPI-10% variable 131 cm^{-1} respectively. Similarly, Barth et al [28] and Guangyong et al [29] suggested peaks at 1319 cm^{-1}, 1327 cm^{-1}, 1346 cm^{-1}, 1379 cm^{-1} similar peaks were observable in the results with peaks at 1328 cm^{-1} for the 0 γ-PGA, 1338 cm^{-1} for the 2.5% γ-PGA variable, 1321 cm-1 for the 5% γ-PGA variable and 1331cm^{-1} for the 10% variable. However, the influence for these peaks were associated with more than 1 potential molecular interaction. For instance, interactions in this region have been associated with COOH in plane bending vibrations, CH_3 wagging vibrations, CH in plane bending vibrations and COO- symmetric stretching vibrations. Potential discrepancies in the comparisons with [28] and [29] could be attributed to differing glutamic acid states utilised in the investigations, i.e. whether the glutamic acid is in a solid form, in a solution or in its pure crystal form. Furthermore, coupled with amino acid interaction with the constituent WPI amino acids the likely attributing to the shift associated in the data presented. Therefore, the results demonstrate the successful incorporation of γ-PGA into the WPI to form viable WPI- γ-PGA hydrogels at the various concentrations.

2.2. Swelling analysis

The results for the swelling assay are shown in Figure 6. The results indicate that the addition of γ-PGA influences the WPI hydrogels in a positive manner, as demonstrated by the increase in the amount of solution the hydrogels can uptake before degrading. However, the result demonstrated that the positive influence of the addition of γ-PGA is concentration dependent. The swelling potential increases from a mass percentage loss of -19.5% for the 0% γ-PGA control to a mass percentage of -7.9% for the 2.5% γ-PGA ($p < 0.05$). However, post 2.5% γ-PGA the hydrogels increased in mass rather than losing mass with the 5% γ-PGA samples gaining a percentage increase of 7.1. However, the 10% γ-PGA sample displayed less swelling potential than the 5% γ-PGA sample, producing a swelling ratio percentage of 4.9% compared to 7.10% ($p < 0.05$).

Due to the novelty of the work featured in this manuscript, there is a lack of literature concerning the effect of the addition of γ-PGA to WPI hydrogels. However, given the hydrophilic nature of the γ-PGA molecule it was expected that the addition of γ-PGA at lower concentrations would positively influence the swelling capacity of the hydrogels, and this is generally observed, with the addition of 2.5% and 5% γ-PGA improving the swelling potential of the hydrogels. Additionally, given that the WPI hydrogels were formed by heat induced gelation and are formed by the initial denaturing of the protein exposing the hydrophobic residues and Sulphur-containing cystine and methionine residues, resulting in homologous hydrophobic interactions and disulphide bridges to form the hydrogel, it would be expected that past a certain concentration hydrophilic and non-Sulphur containing γ-PGA would have a negative effect on the structural integrity of the hydrogels and and result in degradation. Degradation was observable and was the reason behind the decrease in mass observed in WPI/10.A result of the addition of γ-PGA, increasing the non-hydrogel forming amino acid concentration in the hydrogels.

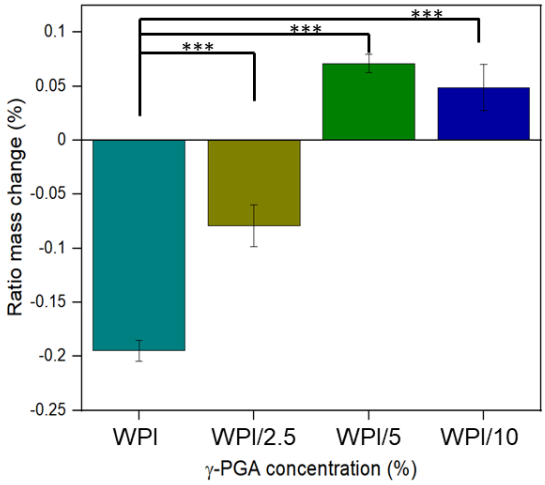

Figure 6. Polymer swelling assay under pH7 conditions. The hydrogel samples were introduced to 5mL PBS solution. Each bar represents the mean ± SD of n=10 (**p < 0.01, ***p < 0.001****p < 0.0001; compared to the WPI control). The observables are γ-PGA concentrations WPI = 0%, WPI/2.5 = 2.5%, WPI/5 = 5% and WPI/10 = 10% γ-PGA.

2.3. Compression analysis

Load bearing potential is a desired property of bone regenerative scaffolds. Therefore, compression analysis was undertaken to ascertain the influence of the incorporation of γ-PGA on the mechanical strength of WPI hydrogels. Statistically significant differences were observed between the sample groups WPI/5 and WPI/10 ($p < 0.05$). However, the incorporation of γ-PGA into WPI hydrogels impacted the mechanical strength of the WPI hydrogels negatively. The results in Figure 7a display a clear concentration-dependent decrease in the load bearing potential of the hydrogels, with an increase in γ-PGA concentration leading to a decrease in strength. Young's modulus decreased from 1200 kPa for the WPI control group to 509 kPa for the WPI/10 sample group, resulting in a 58% loss in structural strength ($p < 0.05$). This result is further supported by the lineal decrease in compressive strength in Figure 7b ($p < 0.05$). The concentration dependence is likely the result of the addition of non-hydrogel forming amino acids diluting the potential for hydrophobic interactions or the formation of disulphide bridges and thus weakening the structural integrity of the hydrogels. Additionally, the WPI hydrogel control group displayed values supported by previous work in literature. The work here produced similar results presented by Ivory-Cousins et al [30] when comparing WPI control samplesThe WPI hydrogel demonstrated a suggested Young's modulus of circa 1200 kPa. However, [30] presented data suggesting an increase in Young's modulus of circa 1300 kPa.

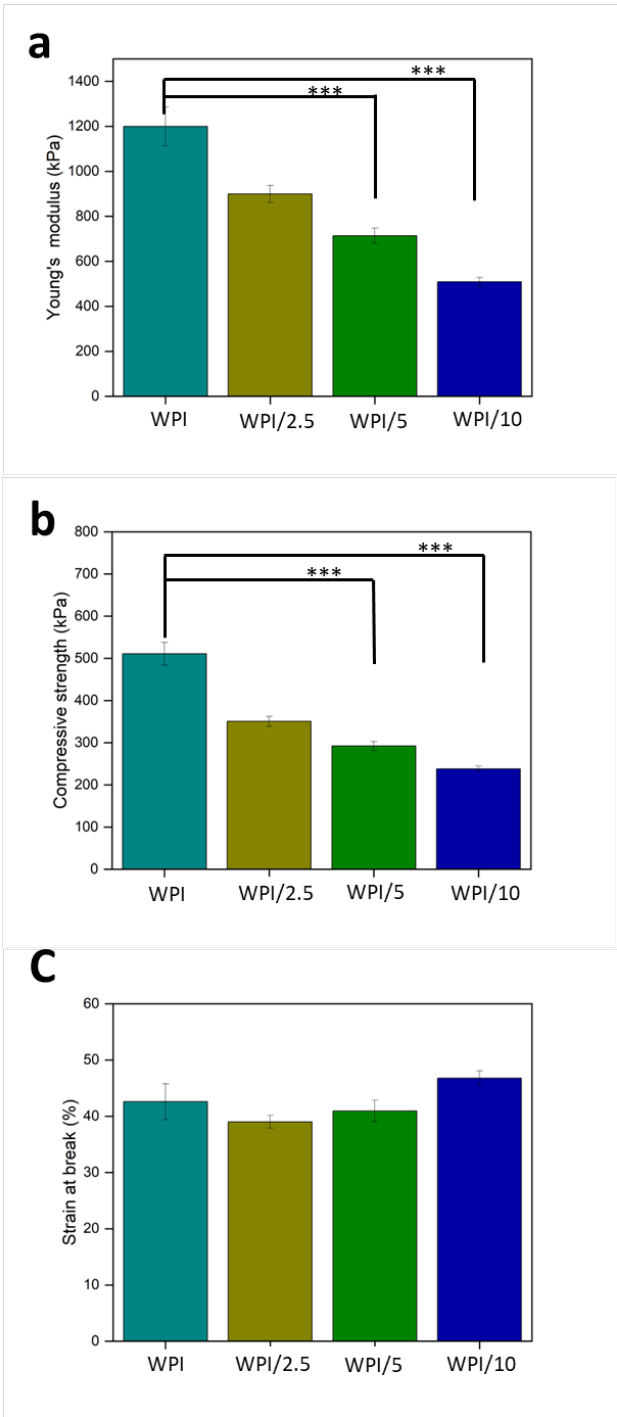

Figure 7. a-c. The results of WPI- γ-PGA hydrogel compression testing. a. Young's modulus, b. Compressive strength and c. % strain at break. Each bar represents the mean ± SD of n=10 (**p < 0.01, ***p < 0.001****p < 0.0001; compared to the WPI control). The observables are γ-PGA concentrations WPI = 0%, WPI/2.5 = 2.5%, WPI/5 = 5% and WPI/10 =10%.

2.4. Biocompatibility and Osteogenic Capacity of the Scaffolds

In vitro biocompatibility of the WPI and WPI- γ-PGA scaffolds was assessed using the PrestoBlue™ cell viability assay from day 3 to day 14, as shown in Figure 8. At day 3, a decrease in cell viability of the γ-PGA -containing scaffolds compared to the WPI control was observed, however, this was not significant. On day 14, a significant increase in proliferation was observed for all three γ-PGA -containing scaffolds compared to the WPI control. Previous studies have recognized the potential of WPI for applications in tissue

engineering, primarily regarding its cytocompatibility [31, 32]. It has been previously reported that the incorporation of γ-PGA as a modifier not only enhanced the structural integrity of a polymer network, promoting material stability, but also fostered hydrophilicity, creating an environment conducive to cell attachment and proliferation [33, 34]. Previous research on dose response of 0.5–0.7 w/v% γ-PGA modified glycerol hydrogels revealed significant enhanced cell proliferation and adhesion compared to the control hydrogels [34]. Another study reported on the significant increase of MC3TE-E1 cell proliferation on γ-PGA scaffolds containing 5 to 20 wt%, from day 1 to day 5 [35].

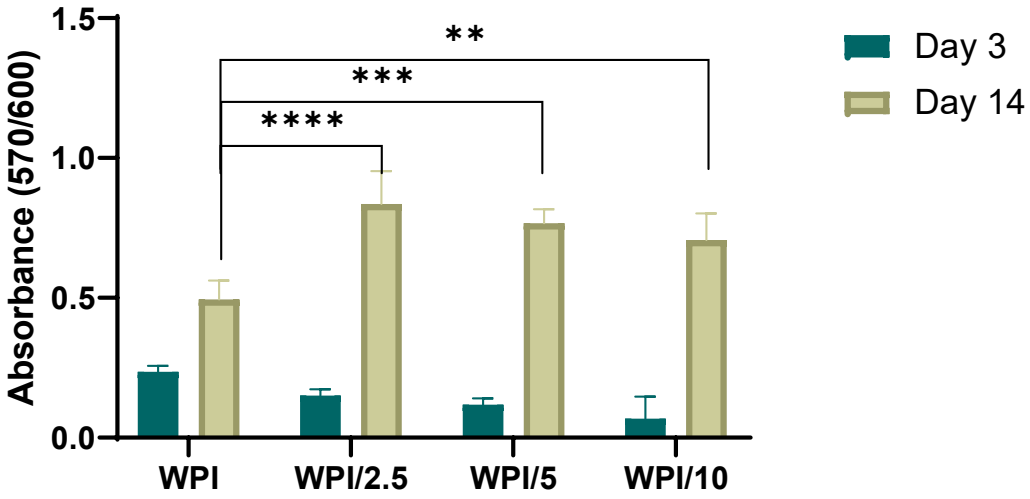

Figure 8. Pre-osteoblastic cell viability and proliferation on WPI and γ-PGA -containing hydrogels of various γ-PGA concentrations at days 3 and 14. Each bar represents the mean ± SD of n=6 (**$p < 0.01$, ***$p < 0.001$****$p < 0.0001$; compared to the WPI control).

Pre-osteoblastic cell adhesion and morphology were evaluated by means of scanning electron microscopy (SEM) imaging after 7 days in culture at x1000 magnification Figure 9). Pre-osteoblasts cultured on all three γ-PGA -containing scaffold compositions exhibit strong attachment. On day 7, the formation of dense layers of cells with their characteristic elongated morphology was observed, as were cell-cell interactions expected to promote tissue formation. Cell nuclei are visible in SEM images of WPI/2.5 and WPI/5, indicating the cell proliferative potential on the scaffolds. All three γ-PGA containing scaffolds displayed stronger cell attachment compared to the WPI control. These results are in line with previous studies investigating scaffolds containing γ-PGA, demonstrating that an increase in γ-PGA content from 0 to 20% w/v promotes cell adhesion [36]

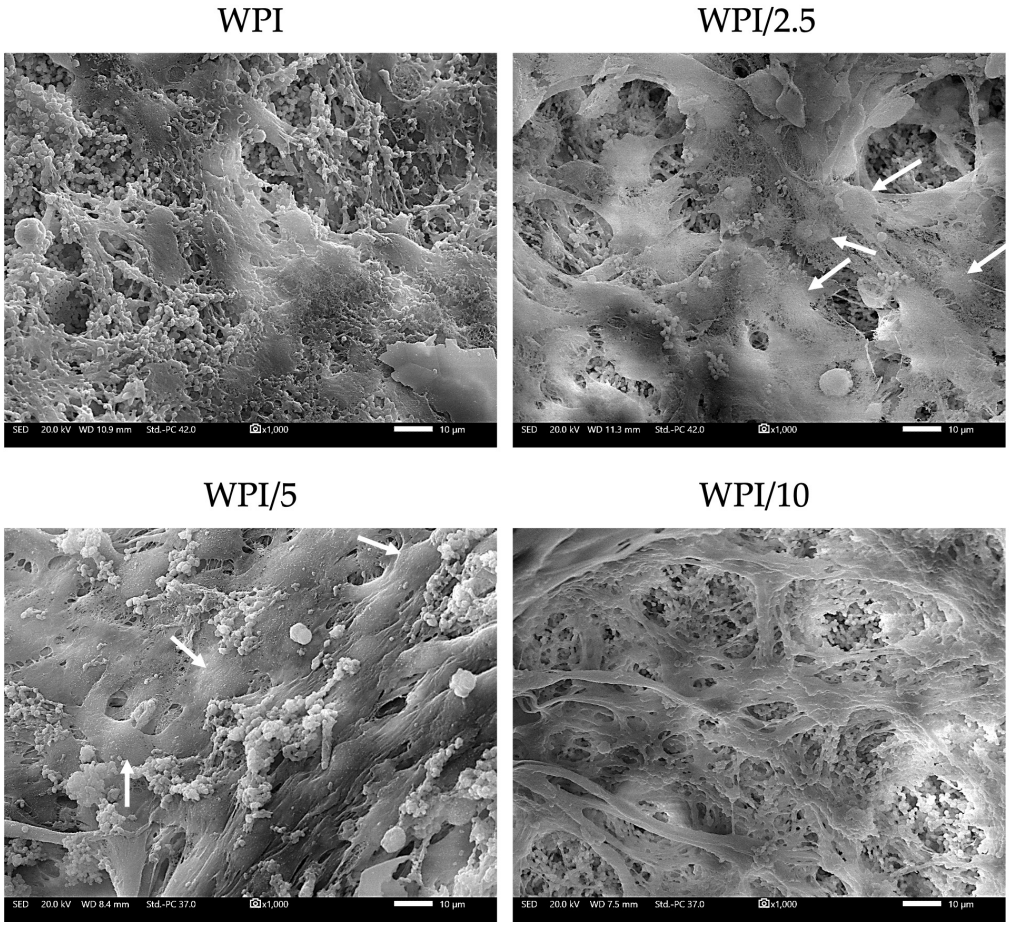

Figure 9. Visualization of pre-osteoblastic cell adhesion and morphology onto WPI- γ-PGA scaffolds with various γ-PGA concentrations on day 7. White arrows point on some visible cell nuclei. Scale bars represent 10 μM, magnification is x1000.

Bone development is a process of continuous deposition of calcium salts, accompanied by increased collagen mineralization. To evaluate WPI- γ-PGA scaffolds as prominent candidates for bone tissue engineering, a comprehensive in vitro study was conducted to assess the scaffolds' osteogenic potential. This involved monitoring of the alkaline phosphatase (ALP) specific activity as an early marker of osteogenesis, calcium production as a late marker of osteogenesis, and quantified the secretion of total collagen, the main structural component of the ECM. Functionalization of WPI hydrogels with γ-PGA induced ALP specific activity at days 3 and 7 at all three concentrations, with a significant 2-fold enhancement for the WPI/2.5 sample group, and a 50% increase for the WPI/10 sample group Figure. 10a. This result confirms the capacity of γ-PGA to promote ALP activity of pre-osteoblasts, which is in line with previously reported [37] data on the use of high molecular weight γ-PGA combined with bone morphogenetic protein 2 enabling its sustained release leading to induction of ALP activity and other osteogenic differentiation markers.

Total collagen levels in the supernatant of the cultured cells on the different WPI- γ-PGA hydrogels were quantified at different time points, as illustrated in Figure 10b. Collagen is a key structural component of the ECM, and deposition of a type I collagen-rich ECM is essential for the expression of specific osteoblasts' products, such as alkaline phosphatase, during the physiological developmental sequence of osteoblasts. The enrichment of WPI hydrogels with γ-PGA resulted in a significant decrease of measured collagen in the supernatants at days 7 and 14. γ-PGA is rich in carboxyl groups, while collagen possesses numerous amino, hydroxyl, and carboxyl groups. Ding et al [39] suggested that

that electrostatic and hydrogen bond interactions between γ-PGA and collagen molecules are paramount for the formation and stabilization of the γ-PGA/collagen bond. This may explain the decreased levels of collagen measured in supernatants of γ-PGA -containing scaffolds. Previously, Bu et al. [39] confirmed this hypothosis experimentally by introducing glutamic acid into collagen solutions, incubated at 37°C. Their results suggested that increasing concentrations of glutamic acid from 50 to 200 mmol/L promoted collagen self-assembly and mineralization, resulting in reduction of collagen levels in solution. Other reports also highlight the effect of glutamic acid on the collagen mineralization process, by promoting collagen self-assembly [40]. Despite reduced collagen related to the presence of γ-PGA, the results in this study demonstrate that collagen production on all WPI-γ-PGA supernatants significantly increased at least four-fold from day 7 to day 21. This gradually increasing collagen secretion by cells suggests active support of ECM formation.

Regarding calcium secretion, a significant enhancement has been observed in all three γ-PGA -containing scaffolds on day 21 compared to the WPI control Figure 10c. The WPI/5 hydrogels showed the highest calcium values compared to all other scaffold compositions on day 14, and significantly higher calcium production compared to the WPI control. From day 7 up to day 21, there was a gradual increase in calcium concentration, indicating that pre-osteoblasts continued their differentiation into mature osteoblasts. Our results agree with other reports describing the excellent apatite-forming ability of γ-PGA due to the presence of carboxyl groups, which are effective for apatite nucleation [41, 42]. Thus, the better deposition of calcium salts could be explained by improved capture of calcium ions by the carboxylic groups of γ-PGA as part of the WPI-γ-PGA. The better osteogenic differentiation of MC3T3-E1 on the surface of WPI-γ-PGA scaffolds is also supported by the specific activity of ALP. All data consistently indicate that the enrichment with γ-PGA enhances the differentiation of pre-osteoblasts into mature osteoblasts and expedites the biomineralization process. Similar improvement in biomineralization has been substantiated in various studies incorporating oligo/poly (Glu). Notably, Karaman et al [43] emphasized the positive impact of glutamic acid peptides bound to PLA/PLGA nanofibers on the nucleation of calcium phosphate and the osteogenic differentiation of bone marrow stromal cells. Averianov et al. [44] observed enhanced in vitro and in vivo biomineralization when nanocrystalline cellulose, modified with poly (Glu), was employed as a filler for PLA or PCL.

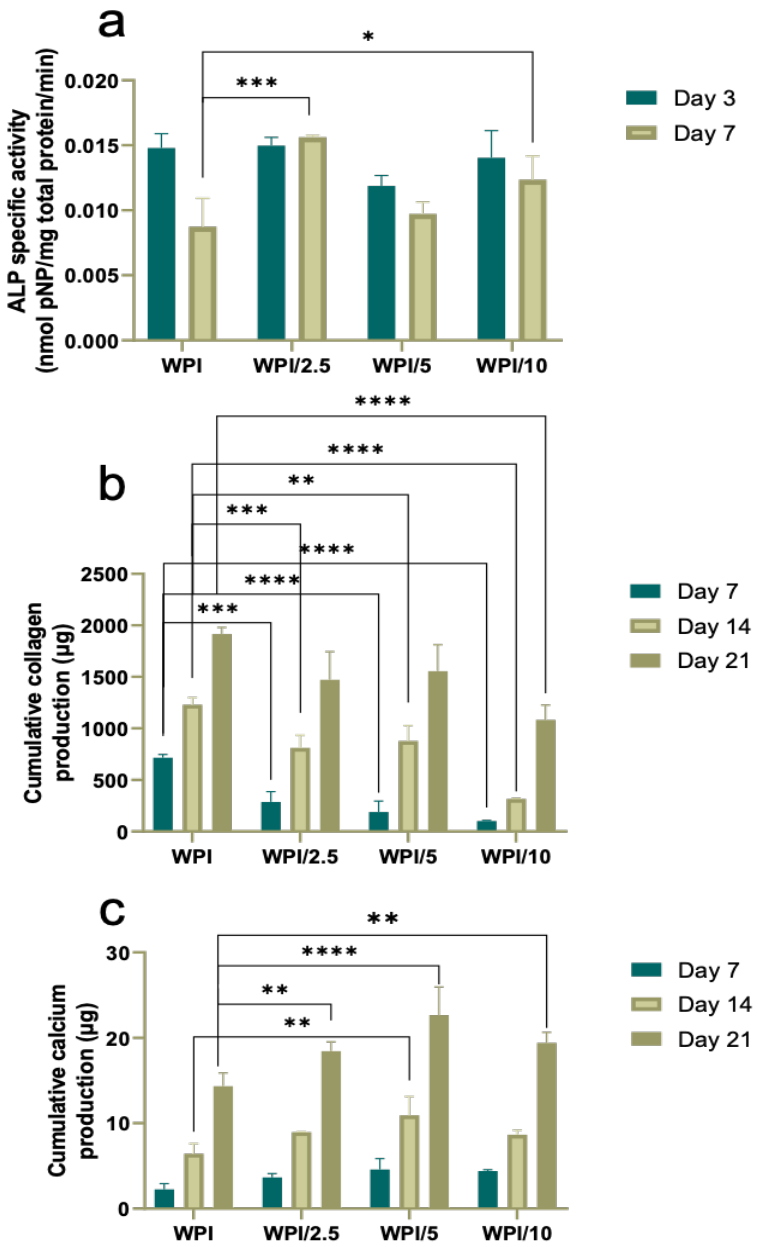

Figure 10. Assessment of the osteogenic potential of pre-osteoblastic cells cultured on γ-PGA -containing hydrogels over a period of 21 days. Expression of normalized ALP specific activity (a), collagen production (b), and calcium production (c) by pre-osteoblasts. Each bar represents the mean ± SD of n=6 (*p < 0.05, **p < 0.01, ***p < 0.001****p < 0.0001; compared to the WPI control).

3. Conclusions

The investigation has demonstrated the successful formation of WPI/ γ-PGA hydrogels. Furthermore, through physiochemical and cellular analysis the investigation provided evidence for the potential of WPI/ γ-PGA hydrogels to be utilised as a novel material for bone regeneration.

Raman spectroscopy demonstrated successful incorporation of γ-PGA into WPI hydrogels, as demonstrated by the observation of concentration dependent linearity in the broadening of the peak at 2928 cm^{-1}. Physical characterisation of the hydrogels was performed; swelling in PBS improved with an increasing γ-PGA concentration. Mechanical testing failed to demonstrate any improvement of the compressive strength.

Based on the biological evaluation results, WPI/2.5 and WPI/5 indicated the highest cytocompatibility values and the formation of a dense cell layer. Particularly, WPI/2.5 displayed the highest ALP activity levels on day 7, and WPI/5 showed the highest calcium production on day 21. Although all three γ-PGA -containing scaffolds supported biocompatibility and osteogenic differentiation of pre-osteoblasts, the two compositions WPI/2.5 and WPI/5 demonstrated the most promising results for bone tissue engineering applications.

Therefore, the investigation suggests WPI/ γ-PGA hydrogels as a primary candidate for further analysis for the purposes of osseous regenerative medicine.

4. Materials and Methods

4.1. Whey protein isolate – poly gamma glutamic acid hydrogel formation.

Whey Protein Isolate (WPI) sourced from Davis and co. Foods international (Minnesota, United States of America) and commercially available poly gamma glutamic acid, with a molecular mass of 440kDa were combined to fabricate hydrogels. The hydrogels were formed under heat induced disassociation. The hydrogels were formed to a concentration of 40% WPI (w/v) with MilliQ H_2O. An additional 2.5%, 5% or 10% γ-PGA was added to create the γ-PGA hydrogel variables. The acquired solutions were vortexed to begin homogenisation before being further homogenised utilising an IKA Loopster for 24 hrs. Gelation was then heat induced at 70°C for 5 min for individual 1 mL samples for analysis formed in 2mL centrifuge tubes. The samples were sterilised by autoclaving. All analyses were performed with sterile hydrogels fabricated by this method. The samples are shown in Figure 11.

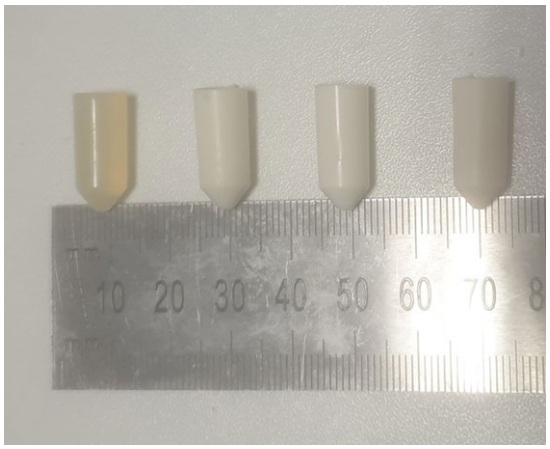

Figure 11. A depiction of WPI-γ-PGA hydrogels post sterilisation in ascending γ-PGA concentration. From left to right WPI, WPI/2.5, WPI/5 and WPI/10.

Table 2. Composition percentages of WPI- γ-PGA hydrogels.

Sample	% WPI	% γ-PGA
WPI	40	0
WPI/2.5	40	2.5
WPI/5	40	5
WPI/10	40	10

4.2. Raman spectroscopy analysis

Raman spectroscopy analysis was utilised to determine the correct incorporation of γ-PGA into the WPI hydrogel. The assay utilised an inVia confocal Raman microscope (Renishaw, Gloucestershire, UK). The hydrogels were introduced to extended spectral

analysis utilising a 785 nm laser by running at 50% power, with a 5 s exposure time and 10 accumulations. The data was analysed on Origin pro peak analysis software. Fitting was achieved using Lorentzian fitting and statistically viability was provided by R-squared values and a one-way ANOVA function.

4.3. Swelling analysis

To determine the both the effect of the structural behaviour of the hydrogels with the incorporation of γ-PGA and the effect of the neutral pH of the osteo environment on the hydrogels, swelling assays were performed. The method was as follows; WPI- γ-PGA hydrogels samples with a mass of 1 g were introduced to a 5 mL pH 7.4 solution, namely phosphate buffered saline. The initial mass of the hydrogels was taken before the samples were incubated for 1 week. The investigation period was chosen to align with previous WPI investigations. Post incubation the final mass was taken, and the swelling mass ratio was calculated using the formula below where the swelling percentage (S%) is calculated from the wet mass (*Mw*) and the dry mass (*Md*)

$$S\% = (Mw - Md)/Md\ x100$$

4.4. Mechanical testing

The potential of hydrogels to be used in an implant environment require load baring potential from the hydrogels. WPI hydrogel present poor load-bearing qualities. Therefore, analysis was compression analysis was conducted to ascertain if the addition of γ-PGA influenced or increase the load-bearing potential of WPI hydrogels. The analysis was achieved through the employment of Instron 3345 (Instron, Norwood, MA, USA). WPI hydrogel sample with γ-PGA concentration percentages of 0%, 2.5%, 5% and 10% were cut to a height of 10mm with a diameter of 8mm. Compressed was achieved at a rate of 2 mm/s.

Youngs modulus E was calculated as $E=\sigma/\varepsilon$ (1) where σ is stress and ε is indicative of strain.

Compressive strength F was calculated as $F=P/((\pi r^2))$ (2) where F is force, P is the load at failure and πr^2 is the area calculation.

Strain at break ε was calculated as $\varepsilon = \Delta L/L$ x100 (3) where ϵ is strain, ΔL is the final length and L the initial length.

4.5. Cell culture and viability

As a model system, an osteoblast precursor cell line MC3T3-E1, derived from mouse calvaria, was utilized for studying cell behavior in vitro when exposed to various scaffolds. Cells at passages 10 to 14 were cultured in a humidified incubator at 37°C with 5% CO_2 in alpha-MEM medium supplemented with 10% fetal bovine serum (FBS), 2 mM L-glutamine, 100 µg/ml penicillin/streptomycin, and 2.5 µg/ml amphotericin. When they reached confluence, the cells were detached using trypsin/EDTA and then seeded onto the scaffolds. Before seeding the cells, the scaffolds underwent a 10-min UV irradiation. A suspension of pre-osteoblastic cells, consisting of 25 × 10^3 cells per scaffold for assessment of proliferation and 40 × 10^3 cells per scaffold for assessment of differentiation, was introduced into the scaffolds in a 10 µl volume of complete medium. Subsequently, 400 µl culture medium were added to each scaffold. The culture medium was changed every three days. For differentiation assays, 10 nM dexamethasone, 10 mM β-glycerophosphate, and 50 µg/ml L-ascorbic acid, were added to the primary culture medium

To assess cell viability, WPI- γ-PGA scaffolds loaded with pre-osteoblastic cells were subjected to the PrestoBlue™ viability assay [42], which utilizes a resazurin-based indicator. This indicator stains living cells upon uptake, producing a red product that can be

photometrically detected. At days 3 and 14 during cell culture, 40 µl of PrestoBlue™ reagent, diluted in alpha-MEM by a factor of 10, were pipetted directly into individual wells, followed by incubation for 60 min at 37°C. Subsequently, 100 µl of the supernatants from the samples were transferred to a 96-well plate, with the help of a Synergy HTX Multi-Mode Microplate Reader (BioTek, Bad Friedrichshall, Germany), absorbance measurements were performed at 570 and 600 nm. The next step was twofold rinsing of the cell-seeded scaffolds with PBS followed by renewal of their culture media. In all experiments, n=6.

4.6. Cell adhesion and morphology evaluation via scanning electron microscopy

Scanning electron microscopy (SEM) was used to examine cell attachment and morphology on the scaffolds. Scaffolds, seeded with MC3T3-E1 pre-osteoblastic cells (25 × 10^3 cells per sample), were incubated in a 37°C incubator with 5% CO_2 for a duration of 7 days. The scaffolds were then rinsed with PBS, fixed for 15 min using a 4% v/v paraformaldehyde solution, and subsequently dehydrated using ethanol of gradually increasing concentrations (ranging from 30% to 100% v/v). Afterward, the scaffolds were subjected to drying in a critical point drier (Baltec CPD 030), coated with an 20 nm thick layer of gold using a sputter coater (Baltec SCD 050), and finally observed under a scanning electron microscope at an accelerating voltage of 20 kV (JEOL JSM-6390 LV).

4.7 Alkaline phosphatase (ALP) activity

To assess ALP activity on days 3 and 7, the scaffolds underwent thorough washing with PBS and subsequent submerging in lysis buffer at pH 10.5 containing 50 mM Tris-HCl and 0.1% Triton X-100. 350 µl buffer was used. Subsequently, a series of three freezing and thawing cycles between room temperature and -20°C were performed. After completion of all three cycles, mixing occurred between a 100 µl suspension of this solution and 100 µl of 2 mg/ml p-nitrophenyl phosphate (pNPP). Prior to mixing, pNPP was subjected to dilution in a buffer which contained 2 mM $MgCl_2$ and 50 mM Tris-HCl. The 200 µl mixture resulting from the previous step was subjected to incubation at 37°C for 1 h Color changes were investigated spectrophotometrically at 405 nm. In order to calculate enzymatic activity, the formula [units = nmol p-nitrophenol/min] was used. Normalization to the total cellular protein in the lysates was performed. The Bradford protein concentration assay was used to determine total cellular protein (AppliChem GmbH, Darmstadt, Germany). For all experiments, n=6.

4.8. Determination of the Produced Extracellular Collagen

The measurement of total collagen levels secreted by pre-osteoblastic cells in the culture medium was conducted using the Sirius Red Dye assay (Direct red 80, Sigma-Aldrich, St. Louis, MO, USA). Supernatants were collected every 3 days, up to day 21, 25 µL of each were diluted in deionized water (dd H_2O) to a total volume of 100 µL, mixed with 1 mL of 0.1% Sirius Red Dye and left to incubate for 30 min at room temperature. Following centrifugation of the samples at 15,000 g for 15 min, the resulting pellets were rinsed with 0.1 N HCl to eliminate any unbound dye. Subsequently, the samples were centrifuged at 15,000 g for 15 min and dissolved in 500 µL of 0.5 N NaOH. The absorbance was measured using a Synergy HTX plate reader at 530 nm. The absorbance measurements were correlated with a calibration curve of collagen type I concentrations. Experiments were performed for n=6.

4.9. Measurement of the concentration of calcium

The O-cresol phthalein complexone (CPC) method was applied for quantification of calcium mineralization as a sign of the development of the extracellular matrix and osteogenesis. [43]. Supernatants were collected every 3 days, up to day 21. In this process, 10 µl of culture medium from each sample were mixed with 100 µl of calcium buffer and 100

μl of CPC calcium dye. The absorbance of these solutions was measured at 550 nm after transfer to a 96-well plate. For all experiments n=6.

4.10. Statistical analysis

Statistical analysis was performed by conducting an ANOVA t-test using GraphPad Prism version 8 software with the aim of determining significant differences between different sample groups and the control at various time points during the experiments. The following p-values were considered to be significant, *p < 0.05, **p < 0.01, ***p < 0.001, ****p < 0.0001, while "ns" means an insignificant difference relative to the WPI control scaffold at the corresponding time point.

5. Patents

Not applicable.

Supplementary Materials: Not applicable.

Author Contributions: The following statements should be used "Conceptualization, T.E.L.D., D.K.B., I.R., M.P., and M.C.; methodology, D.K.B., V.P., M.C, T.E.L.D; validation, D.K.B., V.P., N.N.T., M.C, T.E.L.D; formal analysis, , D.K.B., V.P., N.N.T., M.C, T.E.L.D; investigation, D.K.B., V.P., N.N.T., M.P.; resources, M.C., I.R., K.W. T.E.L.D; data curation, D.K.B., V.P., N.N.T, M.P.; writing—original draft preparation, D.K.B., V.P.; writing—review and editing, all authors.; visualization, D.K.B., V.P., N.N.T., M.P.; supervision, M.C., I.R., K.W. T.E.L.D.; project administration, M.C., I.R., T.E.L.D.; funding acquisition, M.C., I.R., K.W., T.E.L.D. All authors have read and agreed to the published version of the manuscript.

Funding: The Faculty of Science and Technology, Lancaster University, United Kingdom, is thanked for financial support to D.K.B. The research work was supported by the Hellenic Foundation for Research and Innovation (H.F.R.I.) under the "First Call for H.F.R.I. Research Projects to support Faculty members and Researchers and the procurement of high-cost research equipment grant" Project Number: HFRI-FM17-1999 M.C., V.P. and N.N.T.

Institutional Review Board Statement: Not applicable.

Informed Consent Statement: Not applicable.

Data Availability Statement: Data is contained within the article.

Acknowledgments: Molecular graphics and analyses performed with UCSF Chimera, developed by the Resource for Biocomputing, Visualization, and Informatics at the University of California, San Francisco, with support from NIH P41-GM103311.

Conflicts of Interest: The authors declare no conflict of interest. Mattia Parati works for FlexSea Ltd.; however, this company played no part in the design of the study, in the collection, analyses or interpretation of data, in the writing of the manuscript, or in the decision to publish the results, and provided no support, financial or otherwise. The funders had no role in the design of the study; in the collection, analyses, or interpretation of data; in the writing of the manuscript; or in the decision to publish the results".

References

1. Reginster, J.Y. and Nansa B. (2006) "Osteoporosis: a still increasing prevalence." Bone Vol. 38, pages 2-9.
2. Barnsley, J., Buckland, G., Chan, P.E., Ong, A., Ramos, A.S., Baxter, M., Laskou. F., Dennison, E.M., Cooper, C. and Patel, H.P (2021). "Pathophysiology and treatment of osteoporosis: challenges for clinical practice in older people." Aging Clin Exp Res. Vol. 33, pages 759–773.
3. Roseti, L., Parisi, V., Petretta, M., Cavallo, C., Desando, G. and Bartolotti, I. (2017) "Scaffolds for Bone Tissue Engineering: State of the art and new perspectives." Materials Science and Engineering. Vol. 78, pages 1246-1262.
4. Oryan, A., Alidadi, S., Moshiri, A and Maffulli, N. (2014) "Bone regenerative medicine: classic options, novel strategies, and future directions." Journal of orthopaedic surgery and research. Vol. 9, pages 17-18.
5. Yang, Y., Xu, T., Zhang, Q., Piao, Y., Pan Bei, H. and Zhao, X. (2021) "Biomimetic, Stiff, and Adhesive Periosteum with Osteogenic-Angiogenic Coupling Effect for Bone Regeneration." Small. Vol. 17, page 14.
6. Zhang, L., Yang, G., Johnson, B.N. and Jia, X. (2019) "Three-dimensional (3D) printed scaffold and material selection for bone repair." Jia Acta Biomaterialia Vol. 84, pages 16-33.

7. Amini, A.R., Laurencin, C.T. and Nukavarapu, S.P. (2012) "Bone tissue engineering: recent advances and challenges." Crit Rev Biomed Eng. Vol. 40(5), pages 363-408.
8. Hussey, G.S., Dziki, J.L. and Badylak, S.F. (2018) "Extracellular matrix-based materials for regenerative medicine." Nat Rev Mater. Vol. 3, pages 159–173.
9. Giannitelli, S.M., Basoli, F., Mozetic, P., Piva, P., Bartuli, F.N. and Luciani, F. (2015) "Graded porous polyurethane foam: A potential scaffold for oro-maxillary bone regeneration" Materials Science and Engineering. Vol. 51, pages 329-335.
10. Chandra, P.K., S. Soker, S. and A. Atala, A. (2020) "Tissue engineering: current status and future perspectives". Principles of Tissue Engineering. Vol. 5, pages 1-35.
11. Qu, H., Fu, Hongya., Han, Z. and Sun, Y. (2019) "Biomaterials for bone tissue engineering scaffolds: a review" RSC Adv. Vol. 9, pages 26252-26262.
12. Foegeding, E.A., Luck, P. and Vardhanabhuti, B. (2011) "Milk Protein Products | Whey Protein Products." Encyclopedia of Dairy Sciences (2nd Edition), Academic Press, pages 873-878.
13. Wu, J., Chen, H., Zhou, L., Liu, W., Zhong, J. and Liu, C. (2021) "An insight into heat-induced gelation of whey protein isolate–lactose mixed and conjugate solutions: rheological behaviour, microstructure, and molecular forces." Eur Food Res Technol. Vol. 247, pages 1711–1724.
14. A. Abaee, M. Mohammadian, and S. M. Jafari (2017) "Whey and soy protein-based hydrogels and nano-hydrogels as bioactive delivery systems." Trends in Food Science & Technology. Vol. 70, pages 69-81.
15. Dziadek, M., Charuza, K., Kudlackova, R., Aveyard, J., D'Sa, R., Serafim, A., Stancu, I.C., Iova, H., Kerns, J., Allinson, S., Dziadek, K., Szatkowski, P., Cholewa-Kowalska, K., Bacakova, L., Pamula, E. and Douglas, T.E.L. (2021) "Modification of heat-induced whey protein isolate hydrogel with highly bioactive glass particles results in promising biomaterial for bone tissue engineering." Materials & Design. Vol. 205, page 109749.
16. Douglas, T.E.L., Vandrovcová, M., Kročilová, N., Keppler, J.K., Zárubová, J., Skirtach, A.G. and Lucie Bačáková, L. (2018) "Application of whey protein isolate in bone regeneration: Effects on growth and osteogenic differentiation of bone-forming cells," Journal of Dairy Science. Vol. 101(1), pages 20-36
17. Słota, D., Głąb, M., Tyliszczak, B., Douglas T. E. L., Rudnicka, K., Miernik, K., Urbaniak, M., Rusek-Wala, P., Sobczak-Kupiec, A. (2021) Composites Based on Hydroxyapatite and Whey Protein Isolate for Applications in Bone Regeneration. Materials (Basel). Vol. 14(9) page 2317.
18. Gupta, D., Magdalena, K., Tryba, A.M., Serafim, A., Stancu, I.C., Jaegermann, Z., Pamula, E., Reilly, G.C. and Douglas, T.E.L. (2020) "Novel naturally derived whey protein isolate and aragonite biocomposite hydrogels have potential for bone regeneration." Materials and Design Vol. 188, page 108408.
19. Pettersen, E.F., Goddard, T.D., Huang, C.C., Couch, G.S., Greenblatt, D.M., Meng, E.C. and Ferrin, T.E. (2004) UCSF Chimera--a visualization system for exploratory research and analysis. J Comput Chem. Vol. 25(13), pages 1605-12.
20. Bajaj, L. and Singhai, R (2009) "Sequential optimisation approach for enhanced production of poly-gamma-glutamic acid from newly isolated Bacillus subtilis." Food Technology and Biotechnology. Vol. 47, pages 313-322.
21. T. A. Ajayeoba, S. Dula and O. A. Ijabadeniyi (2019) "Properties of Poly-γ-Glutamic Acid Producing-Bacillus Species Isolated from Ogi Liquor and Lemon-Ogi Liquor." Frontiers in Microbiology Vol. 10, page 771.
22. Nair, P., Navale, G.R. and Dharne, M.S. (2023) Poly-gamma-glutamic acid biopolymer: a sleeping giant with diverse applications and unique opportunities for commercialization. Biomass Conv. Bioref. Vol. 13, pages 4555–4573.
23. Poologasundarampillai, G., Yu, B., Tsigkou, O., Valliant, E., Yue, S., Lee, P.D., Hamilton, R.W., Stevens, M.M., Kasunga, T. and Jones, J.R. (2012) "Bioactive silica–poly (γ-glutamic acid) hybrids for bone regeneration: effect of covalent coupling on dissolution and mechanical properties and fabrication of porous scaffolds" Soft Matter. Vol. 8(17), pages 4822-4832.
24. Parati, M., Clarke, L., Anderson, P., Hill, R., Khalil, I., Tchuenbou-Magaia, F., Stanley, M.S., McGee, D., Mendrek, B., Kowalczuk, M and Radecka, I (2022) "Microbial Poly-γ-Glutamic Acid (γ-PGA) as an Effective Tooth Enamel Protect-ant." Polymers Vol. 14(14), page 2937.
25. Yu, Z., Wei, Y., Fu, C., Sablani, S.S., Huang, Z., Han, C., Li, D., Sun, Z., Qin, H. (2023). "Antimicrobial activity of gam-ma-poly (glutamic acid), a preservative coating for cherries." Colloids Surf B Biointerfaces, Vol. 225, pages 113272.
26. Gamarra-Montes, A., Missagia, B., Morató, J., Muñoz-Guerra, S. (2018). "Antibacterial Films Made of Ionic Complexes of Poly (γ-glutamic acid) and Ethyl Lauroyl Arginate." Polymers, Vol. 10, page 21.
27. Freire, P., Moreira B., Alves de Lima Jr, F., José, F., Melo, F., Filho, J. (2017). "Raman Spectroscopy of Amino Acid Crystals." Vol. 10, page 65480.
28. Barth, A. (2000). "The infrared absorption of amino acid side chains". Prog Biophys Mol Biol. Vol. 74(3-5), pages 141-73.
29. Guangyong, Z, Xian, Z., Qi, F, Xueliang, W. 2017."Raman spectra of amino acids and their aqueous solutions" Spec-trochimica Acta Part A: Molecular and Biomolecular Spectroscopy, Vol. 78(3), pages 1187-1195.
30. Ivory-Cousins, T. Nurzynska, A., Klimek, K., Baines, D. K., Truszkiewicz, W., Pałka, K. and Douglas, T. E. L. (2023) "Whey Protein Isolate/Calcium Silicate Hydrogels for Bone Tissue Engineering Applications-Preliminary In Vitro Evaluation." Materials (Basel, Switzerland) vol. 16(19) pages 6484.
31. Platania, V., Douglas, T.E.L., Zubko, M.K., Ward, D., Pietryga, K. and Chatzinikolaidou, M. (2021) "Phloroglucinol-enhanced whey protein isolate hydrogels with antimicrobial activity for tissue engineering." Materials Science and Engineering: C 129 112412.

32. Douglas, T.E.L., Vandrovcová, M., Kročilová, N., Keppler, J. K., Zárubová, J., Skirtach, A.G. and Bačáková, L. (2018) "Application of whey protein isolate in bone regeneration: Effects on growth and osteogenic differentiation of bone-forming cells." J Dairy Sci, Vol. 101(1), pages 28-36.
33. Tong, Z., Chen, Y., . Liu, Y., Tong, L., Chu, J., Xiao, K.,Zhou, Z., Dong, W. and Chu, X (2017) "Preparation, Characterization and Properties of Alginate/Poly (γ-glutamic acid) Composite Microparticles, Marine Drugs, Vol. 15(4), page91.
34. Lin, C.C., Chiu, J.Y., (2021) "Glycerol-modified γ-PGA and gellan composite hydrogel materials with tunable physicochemical and thermal properties for soft tissue engineering application." Polymer, Vol. 230 page 124049.
35. Yang, Q., Zhu, J., Chen, J., Zhu, P., and C. Gao, C. "An injectable bioactive poly (γ-glutamic acid) modified magnesium phosphate bone cement for bone regeneration". Journal of Biomedical Materials Research Part B: Applied Biomaterials n/a(n/a).
36. Kuo, Y.C., and Chung, C.Y. (2012)"TATVHL peptide-grafted alginate/poly (γ-glutamic acid) scaffolds with inverted colloidal crystal topology for neuronal differentiation of iPS cells." Biomaterials, Vol. 33(35), pages 8955-8966.
37. Hu, J., Wang, Z., Miszuk, J.M., Zeng, E. and Sun, H. (2022) "High Molecular Weight Poly(glutamic acid) to Improve BMP2-Induced Osteogenic Differentiation." Molecular Pharmaceutics. Vol 19(12) pages4565-4575.
38. C. Ding, C., Z. Zheng, Z., X. Liu, X., H. Li, H. and M. Zhang, M. (2016) "Effect of γ-PGA on the formation of collagen fibrils in vitro." Connective Tissue Research, Vol. 57(4) pages270-276.
39. Bu, H., Yang, H., Shen, L., Liu, W. and G. Li, G. (2020) "Glutamic acid concentration dependent collagen mineralization in aqueous solution, Colloids and Surfaces" B: Biointerfaces, Vol.190 pages110892.
40. Liu, X., Dan, N. and Dan, W. (2017) "Insight into the collagen assembly in the presence of lysine and glutamic acid: An in vitro study." Materials Science and Engineering: C Vol. 70 pages689-700.
41. A. Sugino, A., T. Miyazaki, T., and C. Ohtsuki, C. (2008) "Apatite-forming ability of polyglutamic acid hydrogels in a body-simulating environment." J Mater Sci Mater Med Vol. 19(6) pages 2269-74.
42. T. Miyazaki, T., Kuramoto, A., Hirakawa, A., Shirosaki,Y. and Ohtsuki, C (2013) "Biomineralization on chemically synthesized collagen containing immobilized poly-γ-glutamic acid." Dent Mater J Vol. 32(4) pages544-9.
43. Karaman, O., Kumar, A., Moeinzadeh, S., He, X., Tong Cui, T. and Jabbar, E. (2016) "Effect of surface modification of nanofibres with glutamic acid peptide on calcium phosphate nucleation and osteogenic differentiation of marrow stromal cells." Journal of tissue engineering and regenerative medicine." Vol. 10(2), pages 132-46
44. Averianov, I.V., Stepanova, M.A., Gofman, I.V., Lavrentieva, A. Korzhikov-Vlakh, V.A. and Korzhikova-Vlakh, E.G. (2022) "Osteoconductive biocompatible 3D-printed composites of poly-d, l-lactide filled with nanocrystalline cellulose modified by poly(glutamic acid)." Mendeleev Communications Vol. 32(6) pages 810-812.